ISBN: 978-3-95450-248-6 ISSN: 2673-5490 doi: 10.18429/JACoW-IPAC2025-MOPS006

THE VACCARO STABILITY DIAGRAM OF SCALING FFAS

D. J. Kelliher*[1], C. Jolly[1,2], A. Oeftiger [2]
[1] STFC Rutherford Appleton Laboratory, UK
[2] John Adams Institute, University of Oxford, Oxford, UK

Abstract

Fixed Field Accelerators (FFAs) are a promising candidate for future high intensity machines such as ISIS-II. It follows that the largely unexplored topic of coherent transverse beam instabilities in these machines is of increasing importance. Transverse instabilities, such as head-tail, can be mitigated in synchrotrons by adjusting the chromaticity appropriately. However, in scaling FFAs, the chromaticity is fixed at zero by design. On the other hand, the relatively strong tune shift with amplitude caused by the nonlinear field of FFA magnets provides a source of Landau damping. Here we evaluate the resulting Vaccaro stability region in the complex tune shift plane comparing an analytical prediction based on the extracted detuning with amplitude with the results from numerical tracking simulations. Hence, the impedance threshold of FFAs can be established.

INTRODUCTION

From the start of their development, the potential of the FFA as a candidate for a future high intensity machine has been recognized [1]. In synchrotrons the repetition rate is limited by the ramp rate of the magnets. This restriction does not apply in the case of FFAs where the magnetic field is fixed, allowing high average beam power. In addition, in FFAs it is possible to accelerate and stack several beams in the machine before extracting, allowing high peak current to be delivered. Recently, an FFA option for a future MW-class neutron spallation source, namely ISIS-II, has been investigated. The study of instabilities in FFAs forms part of this work.

In this paper we focus on transverse coasting beam instabilities. These are of particular interest in the case of beam stacking where a coasting beam may circulate for several acceleration cycles. In this case, even low growth rates may be a concern. Indeed, one of the first experimental observations of a such an instability was made in an early FFA - the MURA 50-MeV electron accelerator [2]. This was soon followed by a paper that laid the foundation of transverse instability theory for the coasting beam case [3].

The nonlinear field in scaling FFA magnets leads to multipoles of all orders. The octupole component results in a linear tune shift with amplitude. This provides a source of tune spread which can damp instabilities. Building on earlier work (e.g. [4]), reference [5] treats Landau damping of collective rigid dipole oscillations in the presence of a two-dimensional betatron tune spread (i.e. including both direct and cross terms in the tune shift with amplitude).

Horizontal scaling FFAs feature a magnetic field scaling as r^k (where k is the field index). Radial sector FFAs achieve vertical stability via F/D magnets, allowing working point adjustment but increasing the circumference due to reverse bending in D magnets. Spiral sector FFAs use edge focusing for vertical stability, avoiding reverse bends but restricting the working point selection and tending to reduce dynamic aperture with spiral angle. FD-spiral sector FFAs offer a third option, combining F/D magnets with spiral edges [7] to achieve a reasonable circumference, fully adjustable working point, and sufficient dynamic aperture.

For the ISIS-II study the FD-spiral FFA is adopted both for the production ring and for its 3-12MeV prototype, the FETS-FFA [8] (named for its injector the Front End Test Stand, FETS [9]) . In this study we take the FETS-FFA as our test case since its design is more advanced. Although this work centers on the FETS-FFA, the analytical techniques and simulation approaches used are general in nature.

THEORY

In the case of a coasting beam and in the absence of tune spread, a transverse dipolar impedance results in a complex coherent tune shift ΔQ_{coh}. In the presence of a transverse tune spread ΔQ_{coh} is modified. Assuming a spread in horizontal tune $Q_x(J_x, J_y)$ the coherent tune shift is given by the dispersion integral

$$1 = \Delta Q_{coh} \int_0^\infty dJ_x \int_0^\infty dJ_y \frac{J_x \frac{\partial \rho(J_x,J_y)}{\partial J_x}}{Q - Q_x(J_x, J_y)} \quad (1)$$

where $\rho(J_x, J_y)$ is the distribution as a function of horizontal action J_x and vertical action J_y. An equivalent dispersion integral applies in the vertical case. Solving Eq. 1 allows a region of stability to be found where a positive imaginary tune shift maps to a zero or negative imaginary tune shift with tune spread.

In general Eq. 1 must be solved numerically. However, an analytic solution exists in the case of a Gaussian beam distribution and assuming linear detuning with amplitude (i.e. corresponding to the tune shift given by an octupole). Following the analysis of Ref. [5], a Gaussian distribution in J_x, J_y is defined as follows

$$\rho(J_x, J_y) = \frac{1}{J_\sigma^4} \exp(-\frac{J_x + J_y}{J_\sigma^2}) \quad (2)$$

where J_σ is the RMS spread of the beam in terms of action. A linear tune shift with amplitude is assumed

$$Q_x(J_x, J_y) = Q_{x0} + aJ_x + bJ_y \quad (3)$$

* David.Kelliher@stfc.ac.uk

ISBN: 978-3-95450-248-6 ISSN: 2673-5490 doi: 10.18429/JACoW-IPAC2025-MOPS006

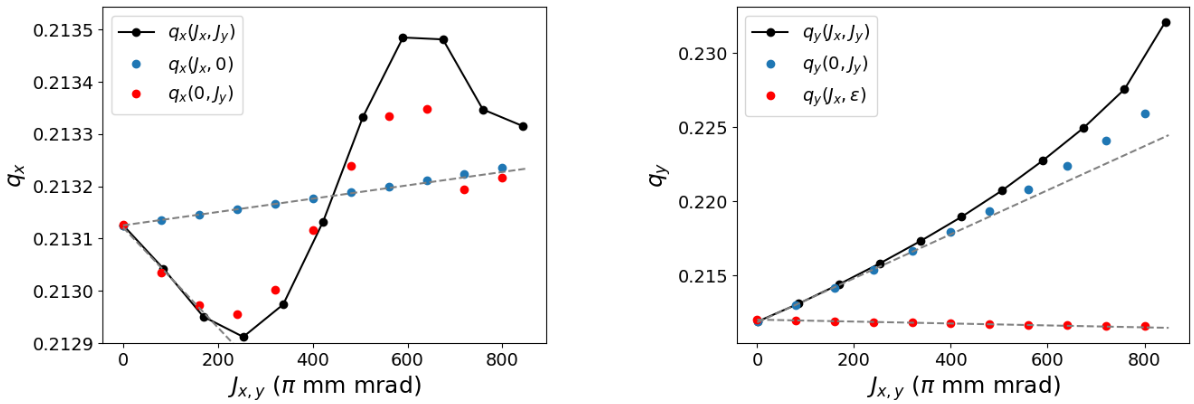

Figure 1: Horizontal (left) and vertical (right) cell tune shift with unnormalised amplitude J_x, J_y. The direct (e.g. $q_x(J_x, 0)$) and cross terms (e.g. $q_x(0, J_y)$) are shown in blue and red, respectively. The tune shift along the line of equal amplitude $J_x = J_y$ is also shown (black). The ϵ denotes a small amplitude added to generate a vertical betatron oscillation when evaluating the cross term in the vertical case. The dashed lines show a linear fit to the first few points. Note the difference in vertical scale between the two figures.

.

where Q_{x0} is the zero amplitude tune and the coefficients a and b depend on the tune shift coming from the direct term and cross octupole terms, respectively. It is convenient to define normalised coherent tune shifts with the RMS tune spread $S = -aJ_\sigma$,

$$q_{coh} = \frac{\Delta Q_{coh}}{S}, \quad q = \frac{Q - Q_{x0}}{S} \tag{4}$$

where q_{coh} and q are the coherent tune shifts without and with Landau damping, respectively. The dispersion integral can be rewritten in terms of q_{coh}

$$q_{coh}(q) = \frac{j}{T(q)} \tag{5}$$

where $T(q)$ is the beam transfer function given by

$$T(q) = j\int_0^\infty dJ_x \int_0^\infty dJ_y \frac{J_x \exp[-(J_x + J_y)]}{J_x + q + cJ_y} \tag{6}$$

where $c = b/a$ is the ratio of the cross term and direct term. The integral can be performed to obtain the solution

$$T(q) = j\frac{1 - c - (q + c - cq)e^q E_1(q) + ce^{q/c}E_1(q/c)}{(1-c)^2} \tag{7}$$

where $E_1(x)$ is the exponential integral $E_1(z) = \int_z^\infty dt \exp(-t)/t$. $T(q)$ allows contours at fixed values of $\mathrm{Im}(q)$ to be drawn in the complex q_{coh} plane (i.e. at fixed growth rates). The area beneath the contour given by $\mathrm{Im}(q) = 0$ is known as the Vaccaro stability region [6]. This approach has been used to calculate the stability region produced by the Landau octupoles in the LHC [10, 11].

FETS-FFA CASE

The lattice parameters used in this study is shown in Table 1. It should be noted that the baseline lattice for the

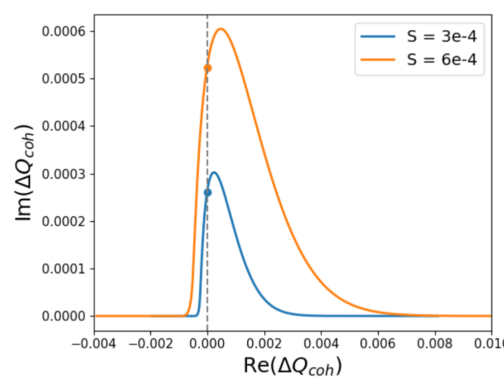

Figure 2: Stability region in terms of coherent cell tune shift ΔQ_{coh} obtained by setting $c = -0.04$ in Eq. 7 and assuming RMS tune spread $S = 3 \times 10^{-4}$ (blue) and $S = 6 \times 10^{-4}$ (orange). The point on each line indicates the stability limit when $\mathrm{Re}(\Delta Q_{coh}) = 0$.

Table 1: Parameters of the 16-Cell FETS-FFA Lattice

Cell type	FD-spiral
Cell opening angle	22.5°
Reference radius r_0	4.00 m
Spiral angle	45°
k-value	~7.7
Opening angle (F,D, short drift)	4.5°, 2.25°, 2.25°
$B_0(r_0)$ (F,D)	~0.34 T, −0.3 T
Cell tune (H,V)	(0.213, 0.212)

FETS-FFA has four-fold symmetry to obtain long drifts. Instead, we assume 16 uniform cells to simplify the lattice specification.

To calculate the linear tune shift coefficients (a, b) in Eq. 3 in the case of the FETS-FFA, a set of single particle tracking

ISBN: 978-3-95450-248-6 ISSN: 2673-5490 doi: 10.18429/JACoW-IPAC2025-MOPS006

Table 2: Linear Tune Shift Coefficients a,b (Eq. 3) in the 16 Cell Symmetric FETS-FFA Lattice Along with the Ratio $c = b/a$

a $(\mathrm{m\ rad})^{-1}$	**b** $(\mathrm{m\ rad})^{-1}$	**c = b/a**
$\frac{\partial q_x}{\partial J_x} = 0.13$	$\frac{\partial q_x}{\partial J_y} = -0.96$	-7.65
$\frac{\partial q_y}{\partial J_y} = 14.86$	$\frac{\partial q_y}{\partial J_x} = -0.65$	-0.04

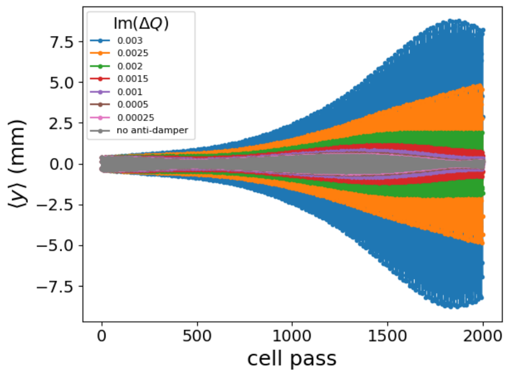

Figure 3: Mean vertical position as a function of cell pass as calculated by Zgoubi combined with the PyHEADTAIL anti-damper. The RMS tune spread S is 3e-4. The gain of the anti-damper is given by the imaginary tune shift. The case where the anti-damper is not included is shown for reference.

simulations are carried out at various amplitudes J_x, J_y from zero up to the dynamic aperture. To improve the accuracy of the tune calculation, the NAFF algorithm is used [12]. The results, in terms of the cell tune shift with amplitude, are shown in Fig. 1. The linear tune shift coefficients are given by the gradient of the fitted lines shown in the figure multiplied by the number of cells. The results are listed in Table 2. The c parameter shown in the table for the vertical case is used to generate the stability region shown in Fig. 2 for the case where the rms tune spread is $S = 3 \times 10^{-4}$ and a factor of two higher.

The predicted stability region can be compared to tracking results by including an anti-damper in the simulation [13]. There are two main approaches to adopt when tracking. In one approach the ring can be represented by a linear transfer matrix with the amplitude detuning term added. Alternatively particles can be tracked step-by-step through the magnetic field of the FFA thereby including the full nonlinear dynamics of the machine. This is the approach we adopt in this paper using the Zgoubi [14] ray-tracking code to do the tracking. After each cell, the bunch coordinates are passed to PyHEADTAIL [15–17] to apply the anti-damper step.

A bunch comprising 1000 particles is tracked through the combined Zgoubi-PyHEADTAIL code for 2000 FFA cells. The RMS action J_σ sets the tune spread via tune shift with amplitude. Here we set $J_\sigma = 25\pi$ mm mrad and $J_\sigma = 50\pi$ mm mrad resulting in RMS cell tune spreads of 3e-4 and 6e-4, respectively (note, the distribution is truncated at 3σ).

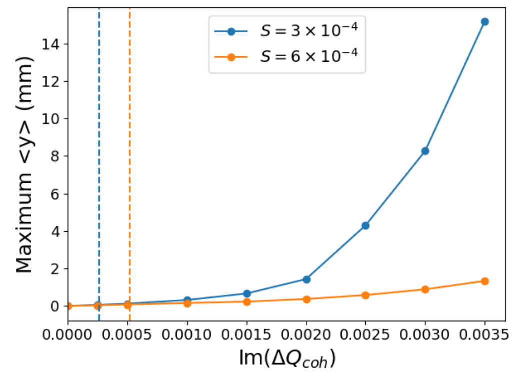

Figure 4: Maximum of the mean vertical position over all cells tracked as a function of the imaginary tune shift for the case where the RMS cell tune spread is 3e-4 (blue points) and 6e-4 (orange points). The baseline case, where no anti-damper is included, is subtracted. The vertical lines indicate the predicted stability limit in both cases (as shown in Fig. 2).

At these J_σ values, the assumption of linear tune shift with amplitude is reasonable (see Fig. 1).

In Fig. 3, the mean vertical coordinate recorded after each cell pass is shown in the case of RMS cell tune spread 3e-4. Tracking is repeated for various anti-damper gain settings. The phase of the anti-damper is 90° in each case, i.e. the real part of the tune shift is zero. It can be seen that even without the anti-damper, the amplitude of the oscillation is not constant. If the bunch isn't uniformly distributed around the closed orbit, the mean coordinate will tend to vary cell-by-cell giving rise to this effect. In the case of the highest anti-damper gain ($\mathrm{Im}(\Delta Q_{coh}) = 0.003$) the instability stops growing after approximately 1800 cell passes. This coincides with an increase in beam emittance, and hence an increase in RMS tune spread, leading to the damping of the instability. This is expected behaviour in machines with nonlinearities.

In Fig. 4, the maximum $\langle y \rangle$ over the course of tracking is shown as a function of $\mathrm{Im}(\Delta Q_{coh})$ when the RMS tune spread is 3e-4 (as in Fig. 3) and when it is doubled. It is clear that the increase in tune spread reduces the growth rate of the instability. The vertical lines show the RMS tune spread in each case. It is difficult to conclude from the tracking results whether these correspond to the stability limit.

CONCLUSION

A preliminary investigation of the stability limit in scaling FFAs has been carried out using Zgoubi as the tracking code together with the PyHEADTAIL anti-damper. In order to determine the threshold of the instability, the effect of the varying bunch centroid due to non-uniformities in the distribution should be addressed. By changing the phase of the anti-damper, the full Vaccaro stability diagram can be explored. It is also of interest to study horizontal instabilities in the same way. Since the ratio of the cross-term to the direct term is large in this case, the stability diagram will look significantly different to the vertical case.

ISBN: 978-3-95450-248-6 ISSN: 2673-5490 doi: 10.18429/JACoW-IPAC2025-MOPS006

REFERENCES

[1] K.R. Symon *et al.*, "Fixed-Field Alternating-Gradient Particle Accelerators", *Phys. Rev.*, vol. 103, p. 1837, 1956. doi:10.1103/PhysRev.103.1837

[2] F.E. Mills, "Coherent Vertical Instabilities in the MURA 50-Mev Electron Accelerator", in *Proc. 1963 Summer Study on Storage Rings, Accelerators and Experimentation at Super-High Energies*, vol. C630610, p. 368, 1963.

[3] L.J. Laslett, V. K. Neil, and A. M. Sessler, "Tranverse resistive instabilities of intense coasting beams in paricle accelerators", *Rev. Sci. Instrum.*, vol. 36, pp. 436–448, 1965. doi:10.1063/1.1719595

[4] D. Möhl and H. Schönaeur, "Landau damping by non-linear space-charge forces and octupoles", in *Proc. 9th Intl. Conf. on High Energy Accelerators*, Rep. CERN-MPS-DL-74-6, p380–384, 1974.

[5] J. S. Berg and F. Ruggiero, "Landau damping with two-dimensional betatron tune spread", Rep. CERN-SL-AP-96-071-AP, 1996.

[6] K. Hübner, A. G. Ruggiero, and V. G. Vaccaro, "Stability of the coherent transverse motion of a coasting beam for realistic distribution functions and any given coupling with its environment", Rep. CERN-ISR-TH-RF-69-23, Geneva, Switzerland, 1969.

[7] S. Machida, "Scaling Fixed-Field Alternating-Gradient Accelerators with Reverse Bend and Spiral Edge Angle", *Phys. Rev. Lett.*, vol. 119, p. 064802, 2017. doi:10.1103/PhysRevLett.119.064802

[8] S. Machida, "FFA design study for a high intensity proton driver". in *Proc. IPAC'23*, Venice Italy, May 2023, pp. 1437–1439 doi:10.18429/JACOW-IPAC2023-TUPA044

[9] A. Letchford et al, "Status of the RAL front end test-stand", in *Proc. IPAC'15*, Richmond, Virginia USA, May 2015. doi:10.18429/JACoW-IPAC2015-THPF105

[10] J. Gareyte, J. P. Koutchouk and F. Ruggiero, "Landau damping, Dynamic Aperture and Octupoles in LHC", LHC-Project-Report-91, 1997.

[11] X. Buffat et al, "Stability diagrams of colliding beams in the Large Hadron Collider", *Phys. Rev. Accel. Beams*, vol. 23, p. 111002, 2024. doi:10.1103/PhysRevSTAB.17.111002

[12] J. Laskar, "The Chaotic Motion of the Solar System: A Numerical Estimate of the Size of Chaotic Zones", *Icarus*, vol. 88, no. 2, pp. 266–291, 1990. doi:10.1016/0019-1035(90)90084-M

[13] S. Antipov et al, "Proof-of-Principle Direct Measurement of Landau Damping Strength at the Large Hadron Collider with an Antidamper", *Phys. Rev. Lett.*, vol. 126, p. 164801, 2021. doi:10.1103/PhysRevLett.126.164801

[14] F. Méot, "The ray-tracing code Zgoubi", *Nucl. Instrum. Methods Phys. Res., Sect. A*, vol. 427, pp. 353-356, 1999. doi:10.1016/S0168-9002(98)01508-3

[15] K. S. B. Li *et al.*, "Code Development for Collective Effects", in *Proc. HB'16*, Malmö, Sweden, Jul. 2016, pp. 362–367. doi:10.18429/JACoW-HB2016-WEAM3X01

[16] A. Oeftiger, "An Overview of PyHEADTAIL", CERN, Rep. CERN-ACC-NOTE-2019-0013. 2019.

[17] PyHEADTAIL is part of the PyComplete repository, https://github.com/PyCOMPLETE.